MEASUREMENTS OF HERA-B RICH TWO-LENS TELESCOPE PROPERTIES. DRAFT # 2.

Reinhard Eckmann, Michael Ispirian, Suren Karabekyan, John McGill, Roy Schwitters, Dan Broemmelsiek

September 1997

1 Introduction

Two aspherical lenses, received from WAHL, were assembled in a telescope. Its properties were studied in an experimental setup.

Part 1: The Setup

2 The telescope

The telescope was assembled from one field lens and one condenser lenses, which were positioned in holders. The holders can slide along three metallic rods running parallel to the optical axis, and their position can be aligned and fixed along the rods. Masks or diaphragms can be put on top of the telescope. In addition, a flat mirror, used for alignment, can be put on top of the field lens.

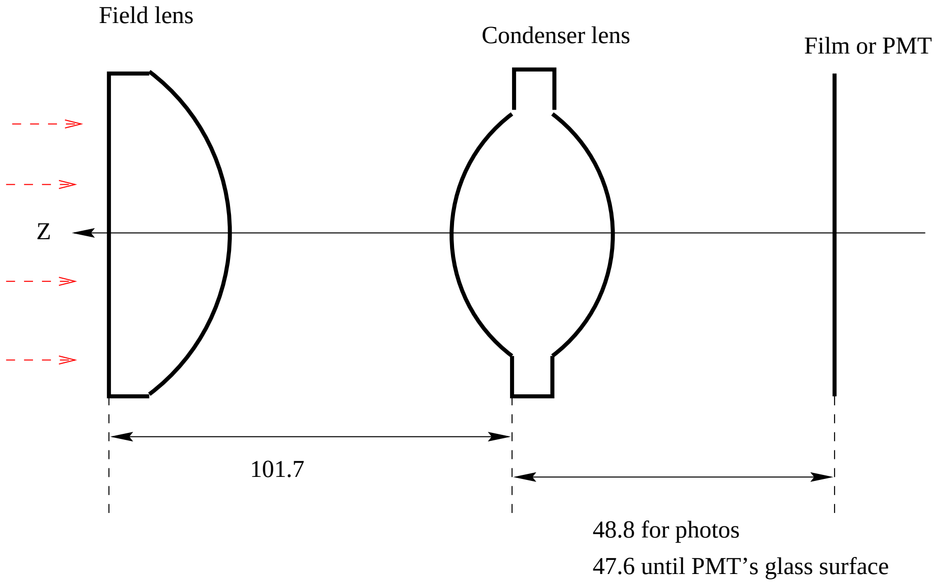

Figure 1: Distances set for telescope studies.

The distances between the lenses of the telescope and the photocathode of the PMT or the film were set to the calculated – optimal for RICH detector – values. Figure 1 shows the set distances.

In the image plane, an M16 photomultiplier tube or photographic film were placed.

The telescope can be removed out of the setup, leaving only the PMT under illumination. This is, in particular, necessary for collection efficiency measurement as well as for study of angular dependencies.

3 The test setup

The telescope with the PMT was placed in a dark box with its axis vertical. Two light sources: a deuterium lamp for UV range and a tungsten lamp for visible range were used as light sources with further filtration through a monochromator. See Figure 2. A detailed description of the light sources and the monochromator is given in the paper "Measurements of Transmission of Plastic." To this setup a "beam parallizer" was added, which provides homogeneous and parallel light beam with diameter 90 mm to illuminate the field lens.

The optics works as follows. The output light from the monochromator is collected with a quartz lens and focused over a diffuser. A small diaphragm right after the diffuser masks the major part of the illuminated area of the diffuser, allowing only 1 mm circle to emit light further. The opening of the diaphragm is in the focal plane of a parabolic mirror, which transforms the light into an almost parallel beam. This beam is then reflected downwards by a flat mirror, illuminating the telescope.

The role of the diffuser is threefold. First, it broadens the angular spectrum, so that the whole necessary aperture of the further optics is filled. Second, the diffuser's output has homogeneous distribution over the lateral coordinate and angular spectrum independent on the angular and lateral homogeneity of the monochromator's output, which makes it possible to obtain a homogeneous parallel beam for the telescope studies. These positive effects of introducing of the dffuser are limited by the third, not desired one: essential decrease of the intensity. To find a reasonable compromise, this small piece of optics was carefully prepared.

The diameter of the output beam is larger than the diameter of the field lens, thus the latter is fully covered. The divergence (angular uncertainty) of the obtained almost-parallel beam is $\approx \pm 2$ mrad. This value is mainly conditioned by the opening of the diaphragm (cannot be smaller since the intensity drops down) and by aberrations of the parabolic mirror.

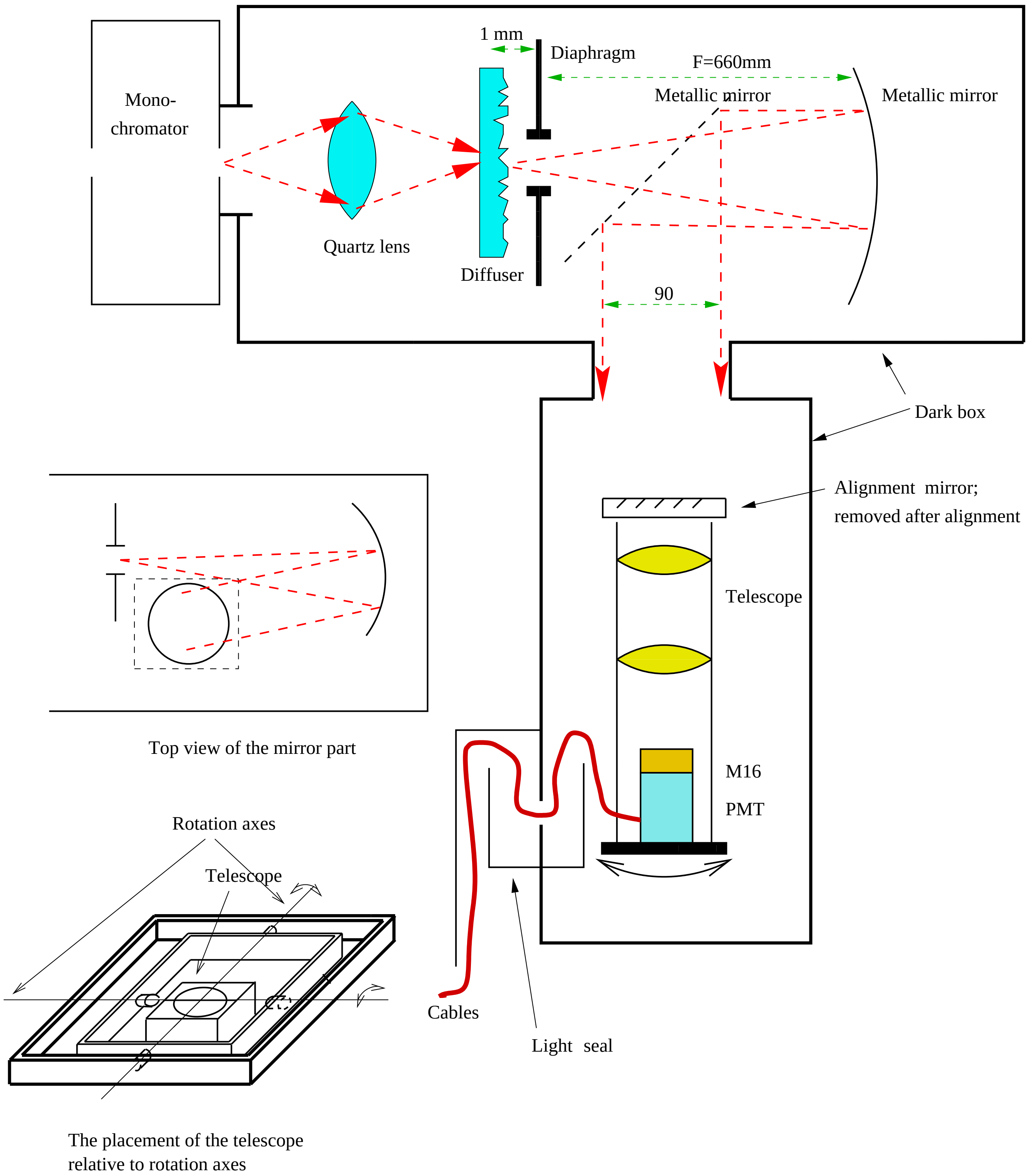

Figure 2: The test setup. Picture is not to scale.

In the dark box, the telescope and the PMT are fixed on a movable platform, allowing rotations along two axes. Declination angles up to $\pm$ 160 mrad are achievable. The uncertainty of the angular position is known with accuracy better than 0.5 mrad.

To minimize the movement of the telescope position during the rotation, the center of the field lens is in the point, where the two rotation axes cross with each other. Thus the spatial position of the field lens center is maintained during the rotation, which prevents it from going out of the illuminating beam.

For the photon detection a Hamamatsu R5600-M16 photomultiplier tube is used. It is plugged into one of 2x1 baseboard prototypes. Two ASD8 boards, necessary to read the signals from one PMT, were used in the setup. The cables from the ASD8 boards run through a labyrinth-like appendix on the wall of the dark box to prevent room light entering the box.

The output of the ASD8 boards is first read by two VME modules, which convert the signals to NIM standard. After, the signals are read by a VME scaler.

For further reference, the numeration of channels of the PMT and the directions of axes are shown in Figure 3.

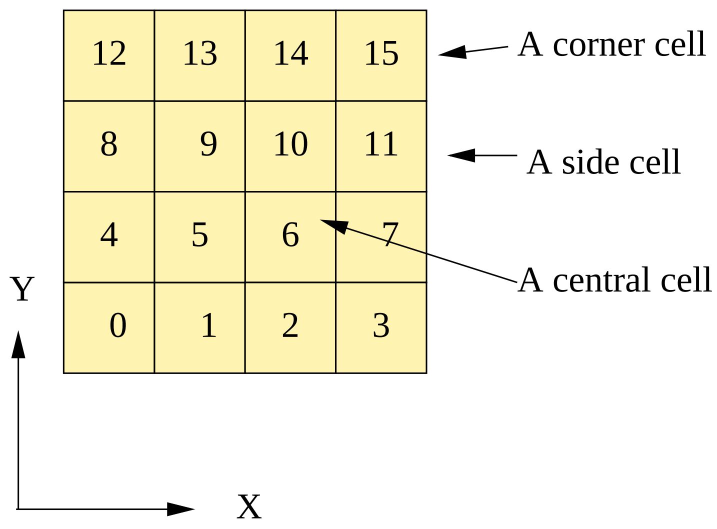

Figure 3: Numeration of channels and direction of axes (not HERA-B coordinate system)

4 Alignment of the setup

The whole setup was aligned relative to incident light prior to the measurements.

The telescope's mechanics was designed in a way, which allows individual alignment of the lenses. The position of the other lens was fixed relative to three rods substituting the telescope's mechanical unity. The positions of the other two lenses and the PMT were set by a caliber and fixed by nuts.

The first alignment of the setup is the centering: assuring, that PMT's center is on telescope's axis. This alignment was done outside the box, by shining a laser beam through a small centered diaphragm placed on top of the field lens and by observation of the spot on the PMT's surface. The body of the tube is shifted until the spot comes to the center of the PMT.

In the next step, the field lens of the telescope was fixed perpendicular to the incident light. This alignment was done by putting a flat mirror on top of of the field lens parallel to the lenses and by observation of the light, which is thus reflected back. The light goes the same path as the incident light, but in the opposite direction, and focuses to a spot in the diaphragm's plane (the diaphragm stands right after the diffuser, see Figure 2). If the mirror is really perpendicular to the incident light, then the spot is inside the opening of the diaphragm and for this reason is invisible. Otherwise, a spot is seen on the right-hand surface of the diaphragm, and the telescope is rotated until the spot appears inside the opening. The parallelism of the middle surface of the field lens and the alignment mirror was achieved through a proper mechanical design of the telescope. This step of alignment procedure was done with laser light, because the monochromator's output is too weak to be seen by eye.

After that the telescope was removed, and the same procedure with the back reflection of the light was done with the PMT: its entrance window was aligned perpendicular to the incident light through shifts in its mechanical holding.

Finally, since the alignments are not quite independent, the steps of alignment were repeated. One–two iterations appeared to be enough. The achieved angular accuracy of the alignment is estimated to be 3 mrad. The lateral misalignment is estimated to be 0.3 mm. This quantity includes the shift of the alignment spot due to lateral shift of lenses in the telescope (shift of the alignment spot is of the same magnitude as the lens shift).

5 Stability of the light sources and of the PMT readout

The basic measurements described further in this paper take from two to twenty minutes to accomplish one step. That for, the long-term stability of the light sources, the PMT and the readout system was studied before the measurements. An alternative could be the usage of a monitor PMT, but the PMT's characteristics themselves as well as the sensitivity of the readout system could drift. Although, a monitor PMT could almost totally remove the influence of the drift of the light sources. However, the setup does not include a monitor PMT, since the one that was initially planned to be used appeared to be defective, and the delivery and preparation time of another would be too long.

Because of drifts, it is desirable to accomplish one measurement as quick as possible. Since the procedure, as a rule, includes opening of the dark box and subjecting of the PMT to daylight, the "rest" characteristics of the PMT was studied: the reduction of the background rate after bright illumination (no high voltage during illumination, naturally). The aim of this study was to find the necessary amount of time one shall wait before data taking after the light sources are switched on or the dark box is opened.

It appeared, that the background resting time is close to 15 minutes, as it can be seen in Figure 4.

If the initial illumination was not bright but rather ordinary room illumination or even attenuated, then the rest time was several times smaller. In all cases, after 10 minutes the mean background rate was less than 40 Hz. Our data on rest time coincides with that brought in the Ljubljana note "Quality assessment tests of Hamamatsu M16 photomultipliers."

There are two main light sources in the setup: a deuterium lamp, covering spectral range 260 – 400 nm, and a tungsten lamp, covering the range 400 – 600 nm. The following Figure 5 shows their stabilities beginning from the moment of switching on. Data taking period is 1 minute. Naturally, the curves represent not only the stability of the photon flux, but also the drift of the PMT's properties and of the further signal processing chain.

Conclusion: the drift over the measurement duration of 20 minutes is smaller than 0.8% after a proper waiting time of 30 minutes.

To monitor the drift, before and after a measurement two reference rates were measured under fixed conditions: one with deuterium lamp and the other with tungsten lamp. An example of a reference measurement is shown in Figure 6. Due to small deviation from constant value, no correction of the measured rates of channels is necessary.

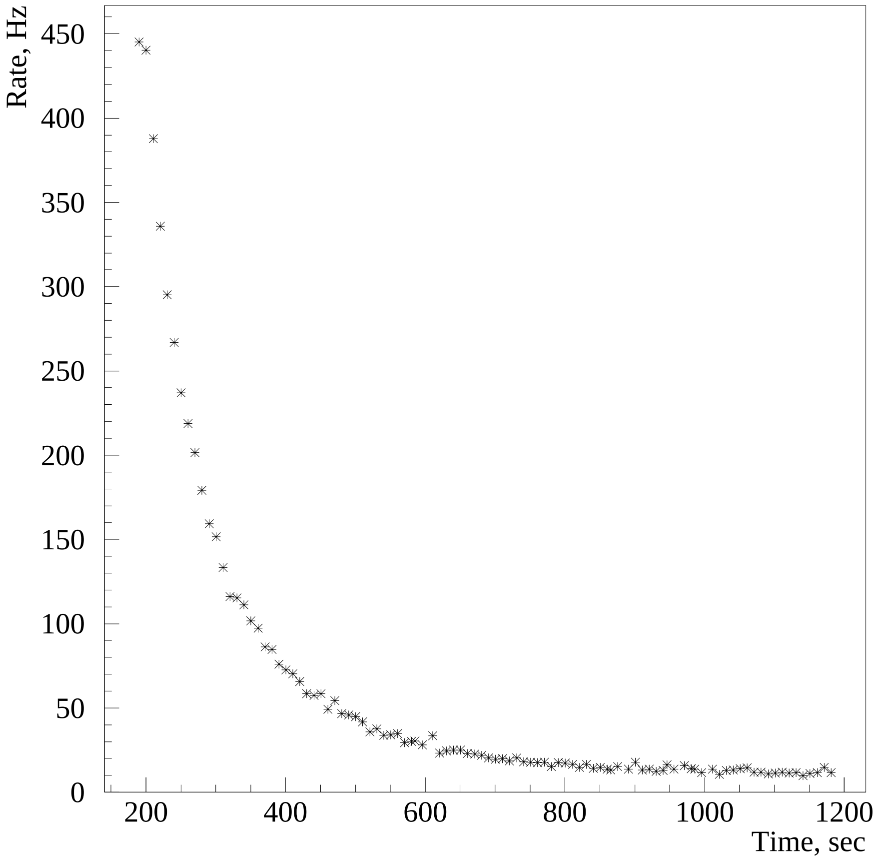

Figure 4: Decrease of the background rate in darkness. Mean rate in channels.

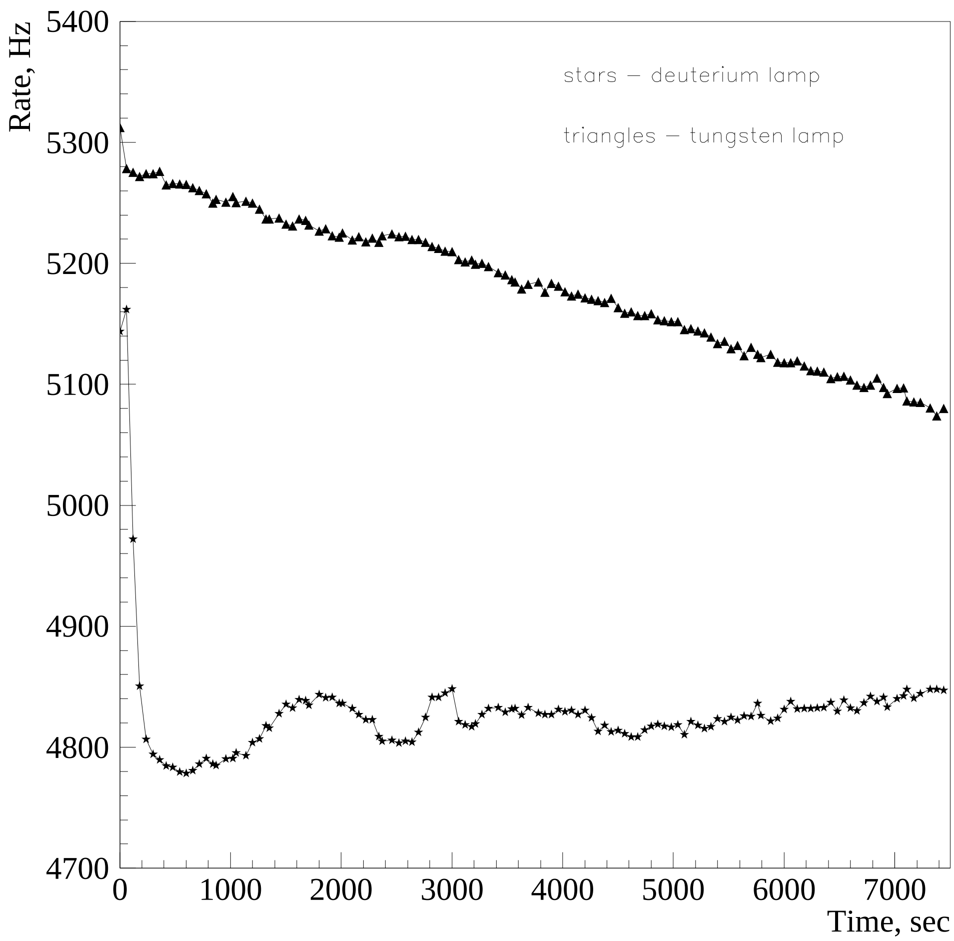

Figure 5: Stability of the two light sources

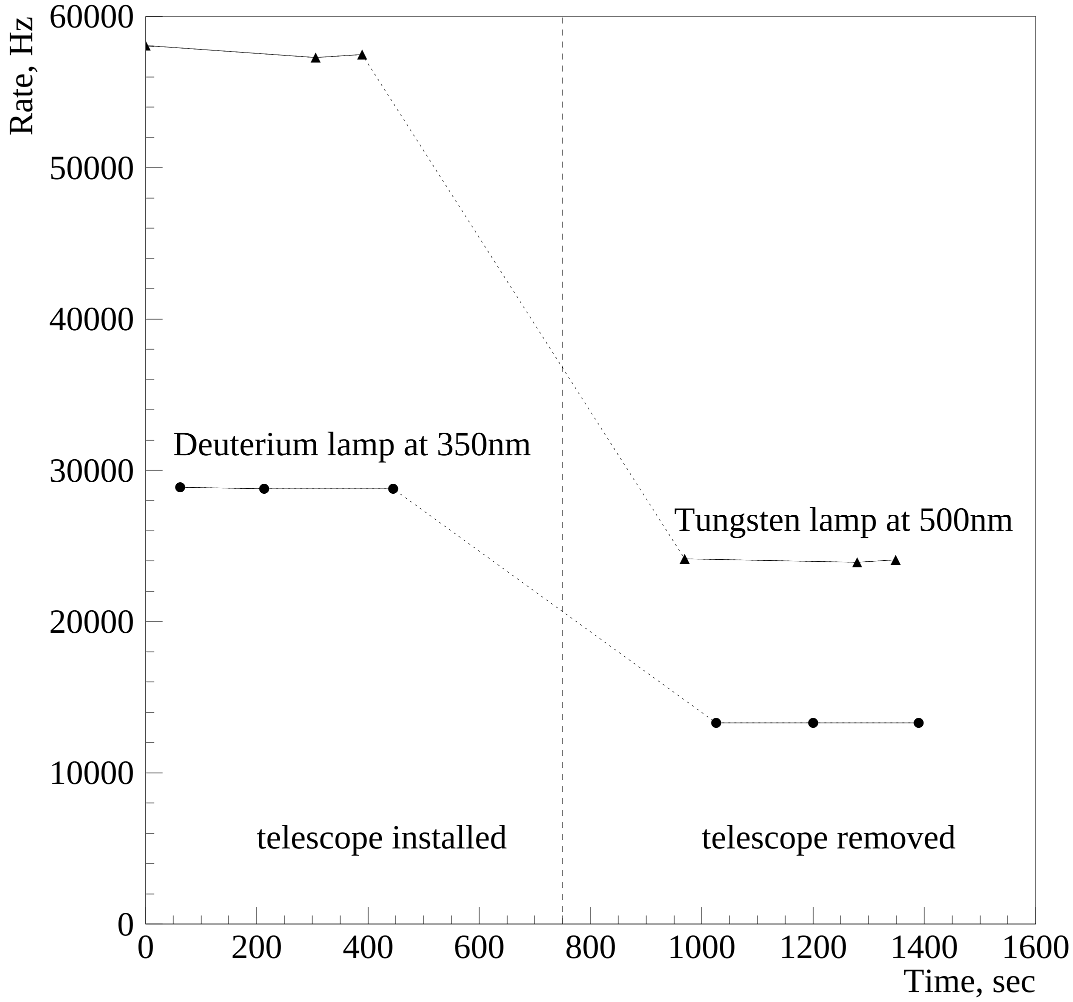

Figure 6: A reference measurement

Part 2: Measurements

6 Test of imaging quality

To estimate the imaging quality of the telescope, the image of a regular grid was photographed directly on photographic film. The grid was placed on top of the flat surface of the field lens. It was made of thin plastic film with black and transparent areas. Two types of grids were used: a dot pattern grid and a concentric ring pattern grid.

With the grid fixed, the setup was illuminated with almost parallel light of a red He-Ne laser (wavelength 632.8 nm), and the incidence angle and the longitudinal position of the film were varied. The following describes the procedures and the results.

The aim of the longitudinal position variation was to obtain the depth of focus and the dependence of the focal position on the radial position of the dot of the grid. The depth of focus, naturally, depends on the angular spectrum of the incident light. For zero incidence angle and parallel rays, the depth of focus appeared to be extremely large: more than 100 mm. The angular spectrum of Cherenkov light was modelled by means of a light diffuser, placed at such a distance, that the angular spectrum of the incident laser light is close to that in the RICH detector. With this angular spectrum, the depth of focus was studied with ring pattern grid installed. Photos will be shown later; here is a short summary. Central and corner areas of the grid have focus at different film positions – approximate difference along the axis is 5 mm. The depth of focus of one spot of the grid is ≈ 0.5 mm.

The aim of incidence angle variation study was to see the deformation of the image at different incidence angles. The longitudinal position was fixed to 48.8 mm as shown in the previous Figure 1. All photos were taken under parallel incident light.

Photos can be found in the ftp are, in the lens_system directory.

One calculation of whether the calculated image and the photographed image coincide was performed. The coincidence looks good. In the Figure 7, black dots show the images od grid's dots and blue circles show the calculated positions of those dots. Pictures are for three different incidence angles.

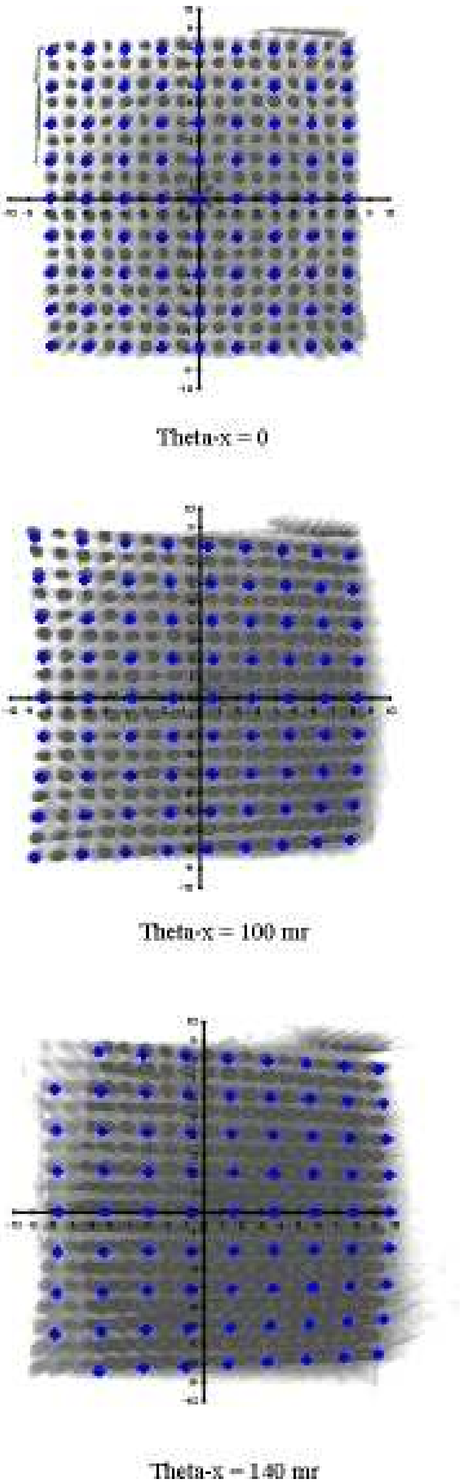

Figure 7: Calculated ant photographed images of the grid

7 Collection efficiency of the telescope over the spectrum

The collection efficiency (transmission) of the channels as well as the mean collection efficiency of all channels was measured by taking the rates with installed telescope and without the telescope. The incidence angle is zero for this measurement. The definition of the collection efficiency we use:

$$Collection\ efficiency\ = \frac{(rate\ with\ telescope)\ -\ (noise\ rate)}{4*((rate\ without\ telescope)\ -\ (noise\ rate))}$$

The factor 4 comes from the nominal magnification factor –0.5.
Collection efficiencies are shown in the following Figure 8.

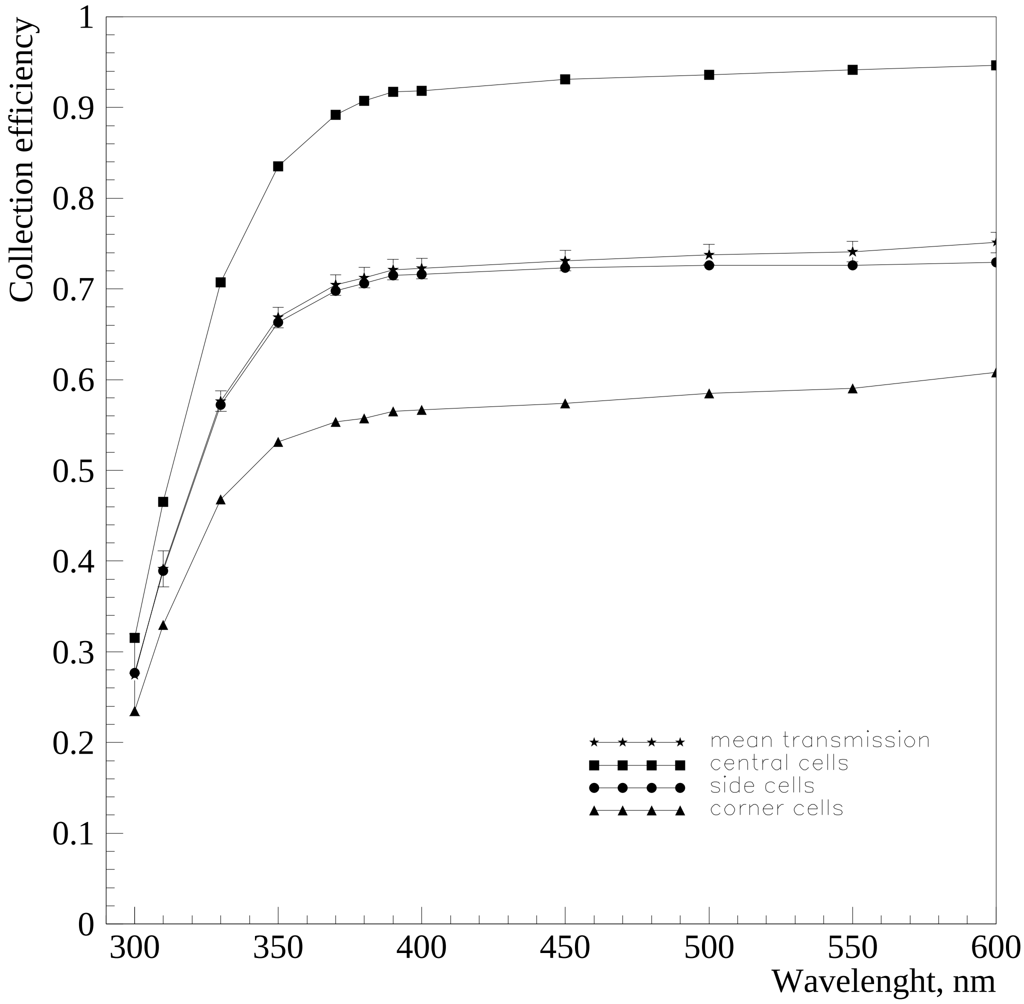

Figure 8: Collection efficiency of the telescope versus wavelength

The instability of the light sources is the dominating error in the collection efficiency measurement. At the wavelengths of measurement 300 and 310 nm the noise (or, to be more exact, the instability of noise) adds its statistical contribution to the measurement error, which is significant only for these two wavelengths. Other errors are much smaller and difficult to estimate. The error bars on the collection efficiency curve in Figure 8 represent the 0.8% lamp intensity drift and the said statistical error, multiplied by $\sqrt{2}$ because the value of collection efficiency is obtained through division of two measurements' data. We do not multiply the 0.8% by 2 but rather by $\sqrt{2}$, because under "error" we understand the standard deviation σ, calculated as sum in squares: $\sigma_{of\ coll.\ eff.} = \sqrt{\sigma^2_{without\ tel.} + \sigma^2_{with\ tel.}} = \sqrt{2} * \sigma_{of\ any\ of\ those}$.

8 Collection efficiency versus incidence angle

The telescope together with the PMT was inclined relative to incident light to study the dependence of the collection efficiency on the incidence angle. Two stepper motors and the rotation mechanics allow to make an angular scan in the range ± 160 mrad in each direction in one run.

The incidence angle over the PMT's surface is approximately twice large, than that over the field lens, and has the opposite sign. That for the angular sensitivity of the PMT was first studied. It appeared, that the sensitivity of the PMT varies within several percents for the angular range of incident light –150 .. +300 mrad and has a maximum not always at zero degree incidence. An example of angular sensitivity is shown in Figure 9. Because of unknown polarization of the incident light and other reasons as well it is difficult to interpret these data.

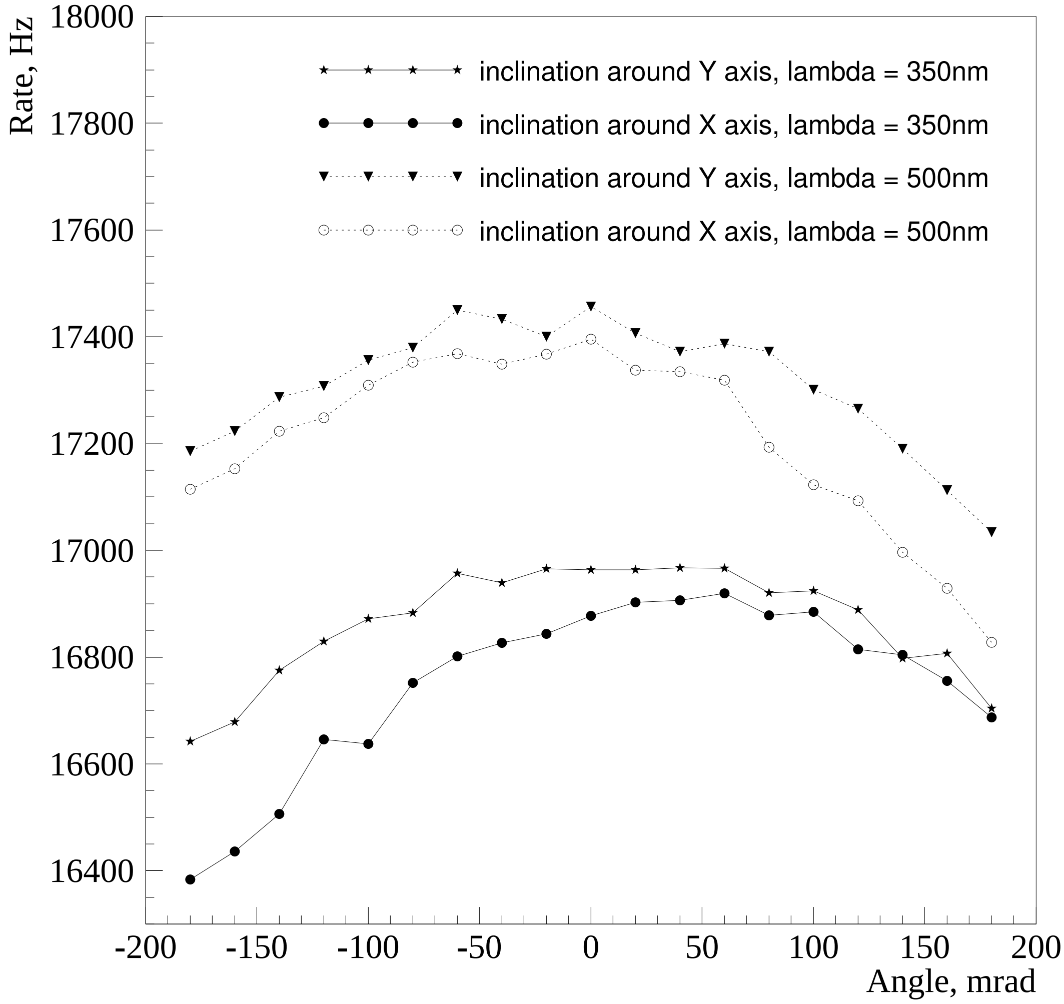

Figure 9: Angular sensitivity of photomultiplier

When calculating the collection efficiency versus incidence angles, the averaged over the whole angular spectrum signals in 16 channels were taken as denominator in the formula for collection efficiency determination, since there is a rather wide angular spectrum falling over the PMT.

In the following three Figures: Figure 10, Figure 11 and Figure 12 the collection efficiency is shown for incidence angles varying in XOZ plane (the rotation axis is Y). Wavelengths are, correspondingly: 300, 350 and 500 nm.

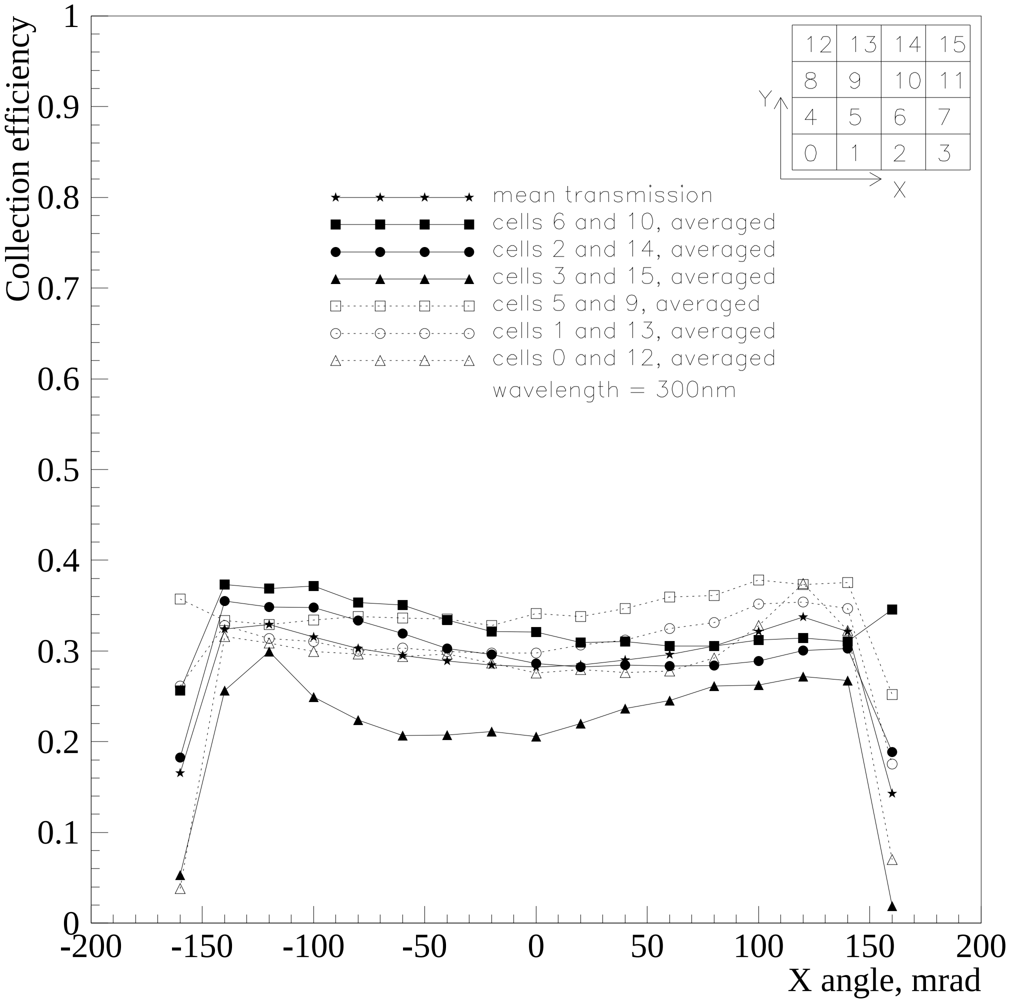

Figure 10: Collection efficiency of the telescope versus incidence angle. Wavelength is 300 nm.

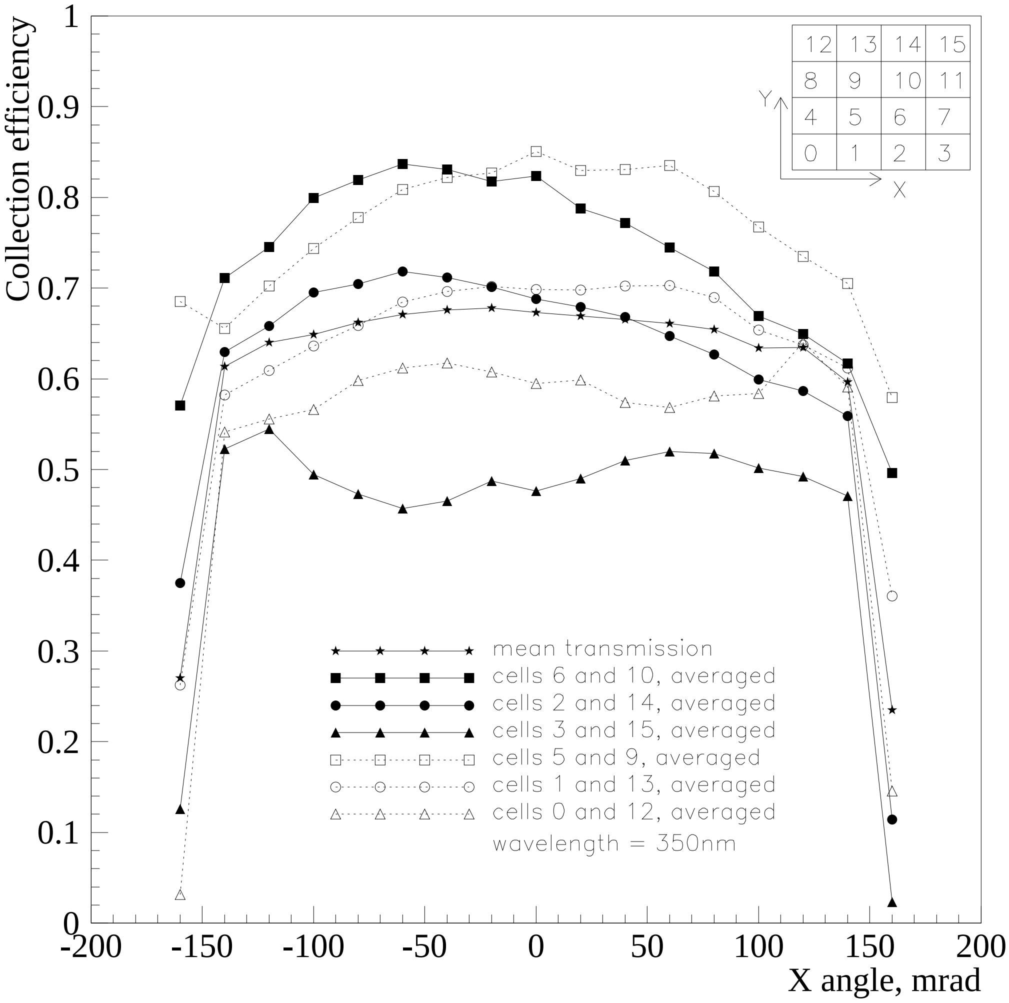

Figure 11: Collection efficiency of the telescope versus incidence angle. Wavelength is 350 nm.

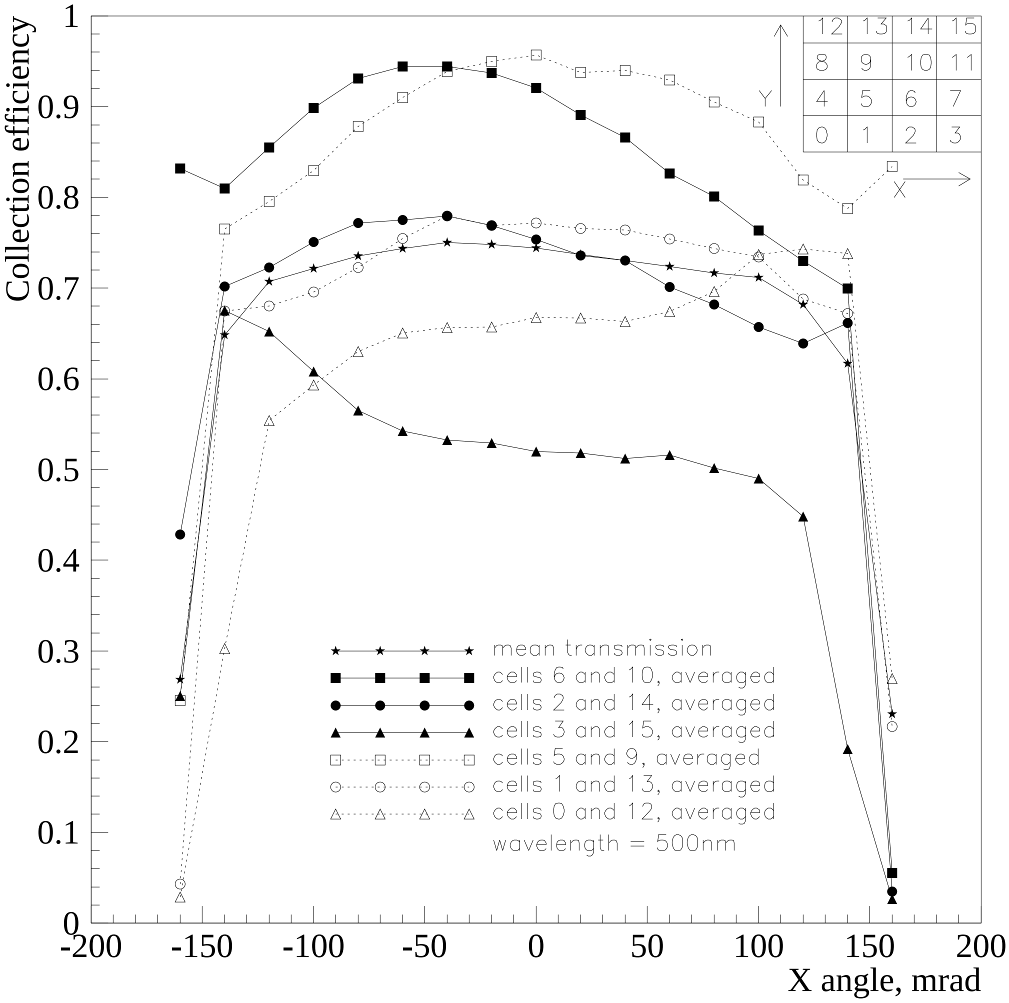

Figure 12: Collection efficiency of the telescope versus incidence angle. Wavelength is 500 nm.

For an ideal telescope, there should be no angular dependence of the collection efficiency. The decrease of the mean collection efficiency with the increase of angle is due to sliding of the whole picture out of the PMT as well as to sharp increase of reflections at the edge of angular acceptance (is clearly seen on the photos). The increase of collection efficiency for some cells is due the shift of the spot, which increases with the angle: when inclined, the cells begin to receive the light, which went to neighbor cells at zero angle. The same crosstalk phenomena explains, why the collection efficiency of some cells is higher than that determined by Fresnel reflections (in absence of absorption and aberrations, four reflections should result in transmission $\approx 0.96^4 = 0.85$).

9 Study of multiple reflections and scattered light

There are five uncoated reflecting surfaces in the setup: four of the lenses and one of the input window of the PMT. Besides, some diffuse scattering of light because of bulk and surface inhomogeneities is observed. That for, a study was performed to estimate the magnitude of reflections and scattered light.

The method chosen was to illuminate the telescope with a narrow beam and register the signals in the channels. In the absence of reflections and scattered light, only signals in the cells, which are directly illuminated with the narrow beam, should be larger than the dark rate. Total number of such cells, evidently, is 1 – 4.

To obtain the narrow beam, a 3-mm diaphragm was placed on top of the field lens. It was positioned so, that at zero incidence angle the image was formed on the cross of the cells # 4, 8, 5 and 9. Thus the position of the spot is known with accuracy ≈ 0.5 mm.

The diaphragm was not positioned on the axis of the lens system, since the reflected photons right in the center go along the same path (because of normal incidence) with the main light and would be thus masked.

The image of the diaphragm on the PMT is ≈ 1.5 mm in diameter. This size could not be further reduced for two reasons: the inhomogeneous sensitivity of the photocathode even within one cell manifests itself too strong, and the absolute intensity becomes so small that the reflections are lost in the noise. The study was carried out at 350 nm, which is thought to be the most important wavelength in the RICH detector.

An angular scan was performed in the range –120 .. +120 mrad.

The results of this study must be treated as approximate only, for several reasons: (i) the amount of registered reflected and scattered light depends strongly on diaphragm position (this statement is also based on visual observation of the reflections with laser beam); (ii) it is not always possible to distinguish between the diffusely scattered and the reflected light; (iii) the signal to noise ratio in not directly illuminated cells is small. However, here are the results.

Study of the scattered light: the illumination through the diaphragm caused a noticeable, although small, increase of background in all channels. Numerically: for the whole scanned angular range, in the mean, the four illuminated cells contain ≈97% of the total rate; the remaining 3% is in the other 12 cells. These 3% include, naturally, not only the diffusely scattered, but also the multiple-reflected photons.

Study of the multiple reflection: for almost all points of the scanned angular range, higher intensity in some 2–4 channels (besides the four directly illuminated channels) was detected. This is, evidently, due to reflections in the optical system. A typical example is shown in the following table, where rates are normalized to the rate in channel # 9 (maximum rate is in this channel), and the individual sensitivity of channels as well as noise level is accounted for. Non-equivalence of signals in channels # 4, 5, 8, 9 is caused by variation of individual sensitivity of the photocathodes (over small are it is rather large) and misalignment of the image of the spot relative to the center of these four cells.

Ch.	Rate	Ch.	Rate	Ch.	Rate	Ch.	Rate
0	0.017	1	0.010	2	0.002	3	0.021
4	0.243	5	0.816	6	0.002	7	0.019
8	0.298	9	1.000	10	0.001	11	0.000
12	0.009	13	0.002	14	0.000	15	0.005

One can see a noticeable increase in rates of channels # 3 and 7. Cell # 0 also has a little higher rate (compare with, say, cell # 13, which is at the same distance from the illuminated cells). When the multiple reflection is estimated numerically, it still lies within the 3%, which occupies the scattered light: as it was said before, the reflections and scattered light cannot be fully separated.

So, the conclusion: the scattered and multiple-reflected photons are observable. Total amount is close to 3%. Reflections are usually observed in 2–4 cells.